REDUCTIVE ELIMINATION

Roald Hoffmann

Department of Chemistry, Cornell University, Ithaca, New York 14853,USA

Abstract - Reductive elimination of an alkane from a transition metal center is a common organometallic reaction, occurring for a wide range of metals, coordination numbers and geometries, and ligands. This contribution presents a theoretical analysis of the reaction, focusing on the options available as the metal and its coordination sphere change.

The coupling of two coordinated alkyl groups into an alkane, 1, is a common step in stoichiometric and catalytic organometallic reaction sequences.

1

This useful reaction proceeds for a great variety of metals, d electron counts and coordination numbers and is especially efficiently accomplished by d^8 transition metal centers such as Ni(II), Pt(II), Pd(II), Au(III). But the simple form of the summary equation 1 masks a multitude of mechanistic choices. Some of these are shown in Scheme 1.

Scheme 1

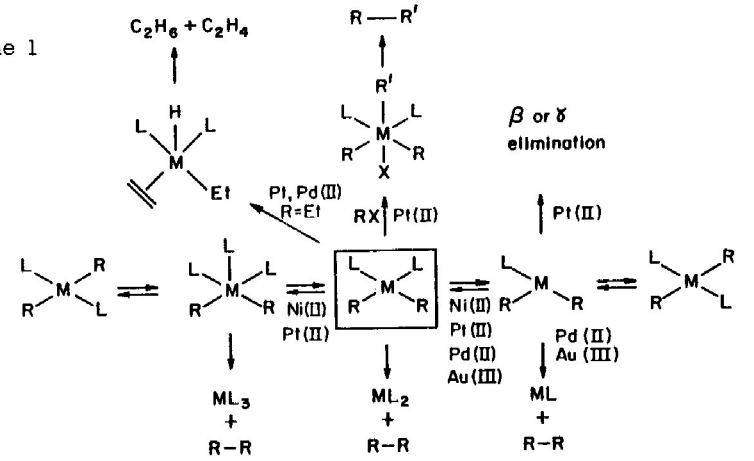

The most common starting point for these reactions is a preformed square-planar 16 electron, d^8 cis dialkyl (or tri-or tetra-alkyl for Au(III)) complex which appears in the middle of the Scheme. The two other ligands, marked L, are typically phosphines. Depending on the size and electronic characteristics of the phosphine substituents one may observe associative or dissociative steps away from the four-coordinate complex. Both elementary processes have been clearly demonstrated in the Grubbs system, where M=Ni(II) and R_2 is a tetramethylene bridge (1). Evidence is in fact in hand for the dissociative step in most such reactions.

The four-coordinate complex eliminates R-R cleanly and easily in the Ni(II) case only. For

Pd(II) the work of the Yamamoto (2) and Stille (3) groups and for Au(III) of the Kochi group (4) has produced kinetic evidence for elimination from a three-coordinate intermediate. Four or three-coordinate Pt(II) apparently does not eliminate R-R readily (5). The Whitesides group (5a) has demonstrated β or γ elimination (where feasible) through a three-coordinate intermediate while Puddephatt and coworkers (6) have found elimination reactions, but only after oxidative addition of an RX. In general the three- and five-coordinate geometries may serve as intermediates for uncatalyzed (7) and ligand-assisted (8), respectively, cis-trans isomerizations of the more stable four-coordinate complexes. Yamamoto and coworkers have shown that the five-coordinate geometry may occasionally be used in elimination in some Ni(II) cases, as well as for some cis and trans Pt(II) and Pd(II) complexes in which a prior β elimination is possible(9).

This briefest summary of much exciting experimental work illustrates that depending on the metal and its coordination sphere, reductive elimination may occur for any coordination number from three to six. An understanding of this largesse has been our goal (10,11,12).

THE FUNDAMENTAL REACTION

One could determine the electronic requirements of each type of complex individually. However it is pedagogically more useful to begin with the "bare metal" reaction, 2. Stepwise accretion of ligands allows a transparent analysis of the changes, essential and nonessential, with d electron count and coordination sphere. Specifically geometries 3-8 have been studied.

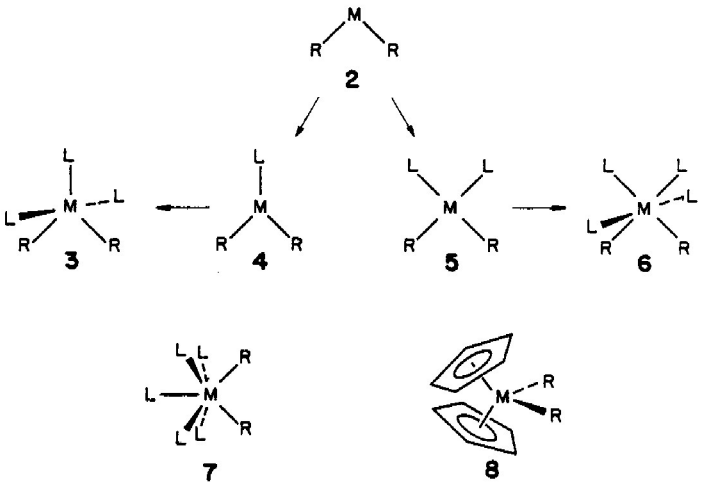

An MR_2 group has two filled metal-ligand σ bonding orbitals, drawn schematically in 9. Both these orbitals are occupied, no matter what the electron count. What happens in the reductive elimination? As the M-R bonds lengthen and the R groups approach each other the a_1 combination, with its two electrons, goes over into the R-R σ bond. This orbital goes down in energy, localizes on the ligands. In the b_2 orbital the ligand-ligand interaction is antibonding. The orbital is saved from correlation to a very high energy σ* orbital of R-R by localization on the metal. These two levels evolve in energy as shown in 10. The (formal) reduction occurs because all four electrons are initially credited to the ligands, while in the end two of them are counted as belonging to the alkane, two transferred to the metal.

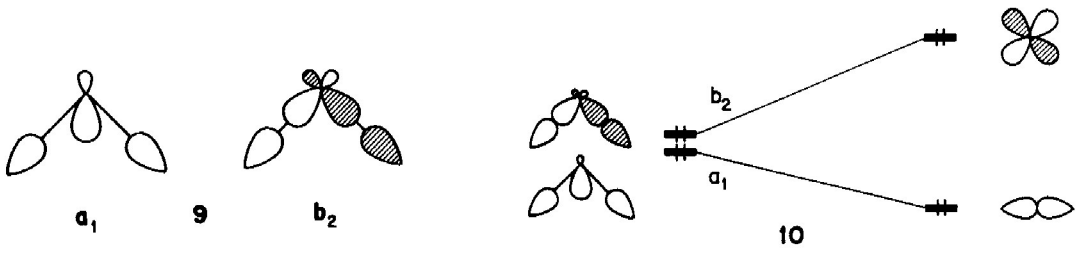

To realize the system one must specify a method of calculation, a molecule, and a reaction coordinate. The procedure we use is the extended Hückel method, a convenient starting point

is M=Pd, R=CH_3. The reaction coordinate, one that has evolved in our studies (8c), simultaneously varies three degrees of freedom defined in 11: the CPdC angle φ, the rocking angle α between the local three-fold axis of the methyl group and the Pd-C bond line, and the Pd-C stretching Δr.

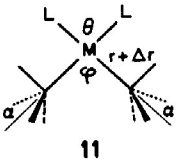

11

The evolution of the energy levels along such a reaction coordinate (specified by φ, α, Δr at the bottom) is shown in Fig. 1. The $1a_1$, $1b_2$, levels are the orbitals previously drawn in 10.

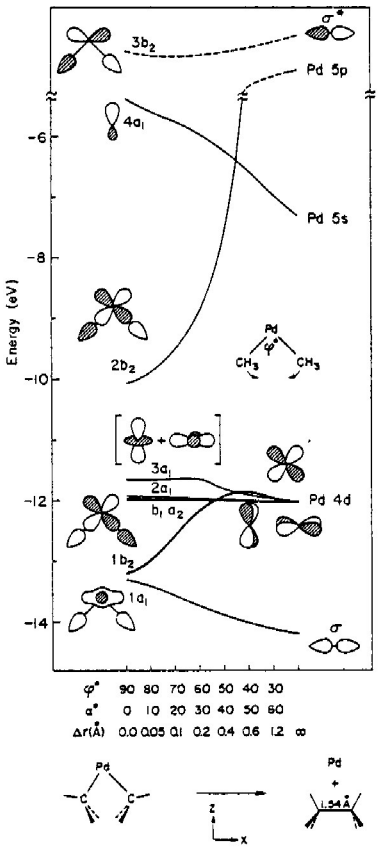

Fig. 1(above) Evolution of energy levels for elimination of C_2H_6 from $Pd(CH_3)_2$. The reaction coordinate is specified at bottom. The dashed line correlations are not to scale. $2a_1$ and $3a_1$ are both mixtures of z^2 and x^2-y^2.

Fig. 2(below). Energy levels and total energy for elimination of C_2H_6 from $LPd(CH_3)_2$ (left) and $L_2Pd(CH_3)_2$ (right). The reaction coordinate is the same as the one specified in detail at the bottom of Fig. 1.

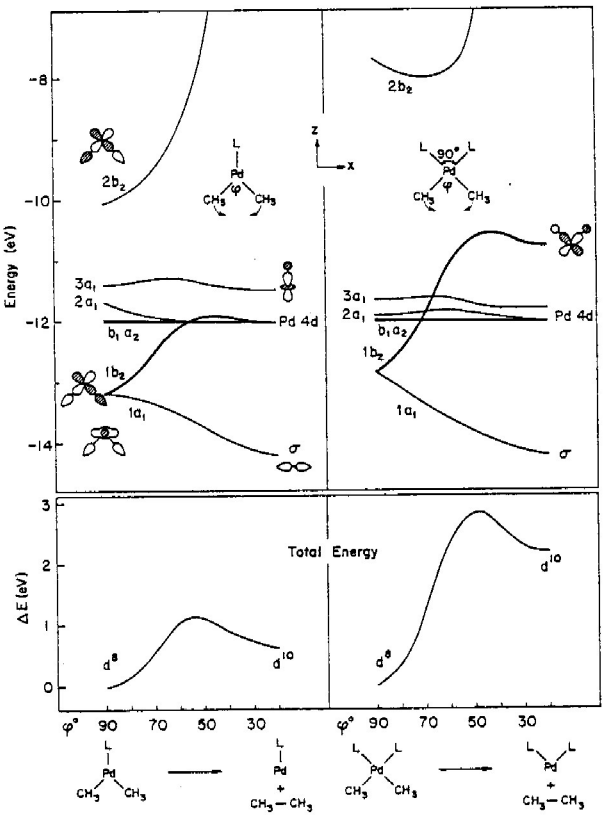

Above them are four metal orbitals little affected by the reaction. Still higher on the MR_2 side are a_1 and b_2 combinations ($2b_2$, $4a_1$, $3b_2$ are shown in Fig. 1) which may be thought of as M-R σ^* antibonding orbitals and virtual orbitals on the metal.

There is not much to say about the reaction. It is symmetry-allowed, i.e. there are no costly level crossings, for $d^8\,MR_2 \rightarrow d^{10}\,M$. The activation barrier is provided by the $1a_1 - 1b_2$ differential, and as usual the higher orbital, $1b_2$, dominates.

Let us bring in one or two ligands, to form the important three- and four-coordinate geometries 4 and 5. This is done in Fig. 2 for a ligand L which has no π-bonding capability. L is a hydrogen atom whose 1s orbital energy is set equal to the calculated energy of a lone pair of a model phosphine, PH_3.

The single ligand in Fig. 2 left interacts primarily with a high-lying a_1 orbital of ML_2, a hybrid of primary s, p character directed toward L ($4a_1$ in Fig. 1). The only change in the valence region is a slight destabilization of $3a_1$, mainly z^2 on the metal. Otherwise the perturbation is minimal. The reaction is allowed for a d^8 electron count in ML_2.

The two ligands in Fig. 2 right interact primarily with high-lying a_1 and b_2 combinations of ML_2 ($4a_1$ and $3b_2$ in Fig. 1). They destabilize slightly $3a_1$ and somewhat more $2b_2$ on the ML_2 side. But much more significant is what happens to $1b_2$. It rises above the d block early in the reaction and remains above it at the end. The behavior of this level is crucial for it leads to an important characteristic of the reaction: Reductive elimination is in general easier from a three-coordinate then from a four-coordinate d^8 complex.

This result fits the bulk of our experimental experience (1-5,9) yet it is counterintuitive. In a reaction which overall lowers the electron count at the metal the 14 electron complex is more reactive than the 16 electron complex. It's important then to probe further for the origins of this effect.

It might be reasoned that the high position of $1b_2$ on the right side of Fig. 2 right (relative to Fig. 2 left) is due to the 90° angle maintained in LML. In other words we have not allowed the LML remnant to relax to its perhaps preferred geometry. Let us do so, incorporating into our reaction coordinate the opening up of the LML angle θ as R_2 departs. The valence orbitals and total energies with and without relaxation are compared in Fig. 3.

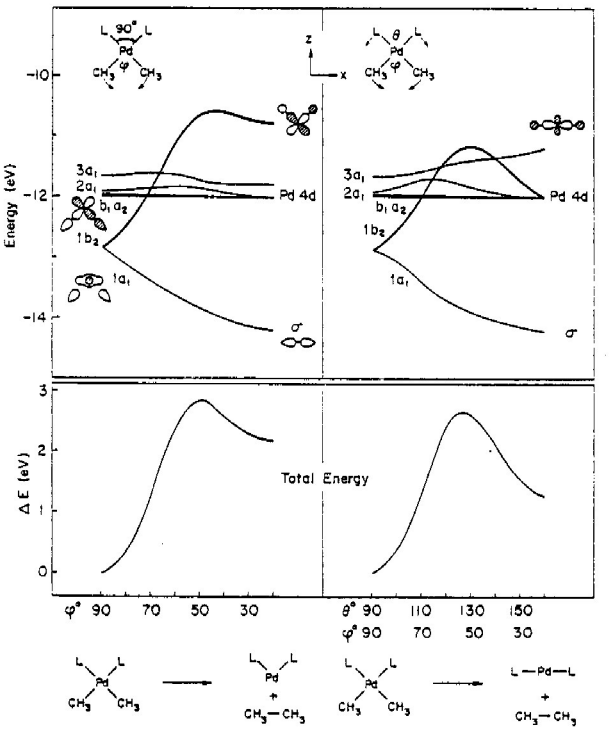

Fig. 3. Frontier orbital energies (top) and total energies for a d^8 configuration (bottom) of $L_2Pd(CH_3)_2$ undergoing reductive elimination. At left the L-Pd-L angle θ is kept at 90°. At right it is allowed to relax along the reaction coordinate.

As the LML angle opens $1b_2$ returns to its nonbonding, pure d character near the end of the reaction. Something is gained, not as much as one might have thought, for instead an a_1 orbital is destabilized in the linear ligand field. But most importantly the reaction barrier remains high, and it does so because in the transition state region, $\varphi \sim 50\text{-}60^\circ$ the b_2 level still rises above the d block.

Why does the b_2 level go up so high in the intermediate stages of the reaction? One way to reason about this phenomenon is as follows:

1. There are two factors governing the rise in energy of b_2. First there is the R····R antibonding interaction in it which would increase along the reaction coordinate. Second, and inextricably connected to the first factor, is the localization of b_2 along the reaction coordinate, 12, by which a metal-ligand bonding orbital is converted into a metal nonbonding level.

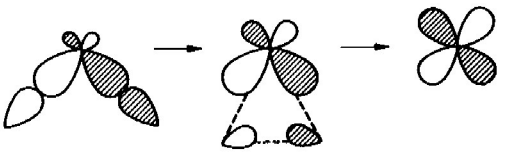

12

2. The two extra ligands L mix into $1b_2$ in an antibonding way, as in 13. That mixing is minimized in the initial four coordinate geometry, for there $1b_2$ is primarily tied up in M-R bonding.

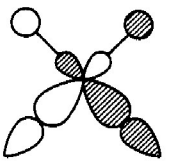

13

3. If L-M-L were not to open up as the reaction proceeds then the LM antibonding would be very much destabilizing in the product. The L-M-L angle opens up to alleviate this problem, 14, but not fast enough. The "rate" of L-M-L opening is constrained by the four-coordination.

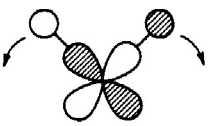

14

If the L-M-L angle were to open up more quickly there would occur repulsive interactions with the leaving R groups.

It might be noted that in our previous analysis of the four- vs.three-coordinate elimination (10a) we dealt with Au(III). There the metal d orbitals are substantially lower, and metal contribution to the b_2 orbital is mainly p rather than d. This changes the shape of the orbitals, but not the essence of the analysis.

Let us return to the general analysis and build up trigonal bipyramidal and octahedral geometries 3 and 6 by adding two ligands axially along the y direction to the trigonal and square planar complexes of Fig. 2. The two additional ligands form combinations of a_1 and b_1 symmetry, 15. b_1 interacts with a metal p, and a_1 interacts, strongly so, with one of the d block a_1's. The net result, not illustrated here, is that the d block orbital, z^2, is pushed up in energy away from the d block. Otherwise the orbital and total energy profiles (now $d^6 \rightarrow d^8$) are virtually identical to those shown in Fig. 2 and 3.

The six-coordinate reaction is thus allowed but difficult for d^6, the five-coordinate one allowed but easier for the same electron count. Once again the more coordinatively unsaturaturated

geometry has an easier elimination channel.

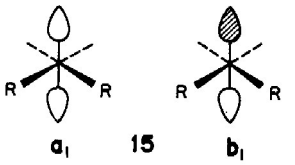

It is just as easy to analyze the seven-coordinate geometry 7 and find that elimination from the unique edge of a capped trigonal prism is nicely allowed for a d^4 electron count (13). Is anything forbidden? Well, just a few things are. One of them is reductive elimination from a 16 electron d^0 Cp_2MR_2 complex, 8. While there is a rich chemistry of such complexes direct elimination indeed does not seem to take place.

Now that we have developed a simple picture of the electronic requirements of the reaction let us turn to the role of the metal and the substituents it bears.

REDUCTIVE ELIMINATION FROM CIS FOUR-COORDINATE COMPLEXES

We return to the most common point of departure for reductive elimination, the square planar d^8 complex, and inquire first what is the origin of the dependence of the activation energy on the metal. Direct elimination appears to be easy for Ni, more difficult for Pt, Pd. First of all this was confirmed by detailed calculations for Ni and Pd. The subsequent tracing of the effect was made simpler by moving to a "hydride model". Here the ligands were simply hydrogen 1s functions with modified valence state ionization potentials. We called the two extremes A and D. A and D are hydrogen atoms, the 1s orbital energies of which are set to be -14.34 eV and -11.75 eV, respectively. The value -14.34 eV is the calculated orbital energy of a lone pair in PH_3 and -11.75 eV corresponds to that of a lone pair in CH_3^-. Thus A^- may be a model for PH_3 and D^- for CH_3^-. Or one can regard A as a poor donor ligand and D as a strong donor ligand.

The Walsh diagrams for D_2 elimination from Pd $A_2D_2^{2-}$ and $NiA_2D_2^{2-}$ are compared in Fig. 4. The computed barriers to elimination are 0.65 eV for Pd, 0 for Ni. The contrast between the potential energy surfaces for the two metals arises from the difference in slope of the $1b_2$ orbitals. As φ decreases $1b_2$ of Pd $A_2D_2^{2-}$ is significantly more pushed up than that of $NiA_2D_2^{2-}$, producing an energy barrier in the elimination of D_2 from the Pd compound.

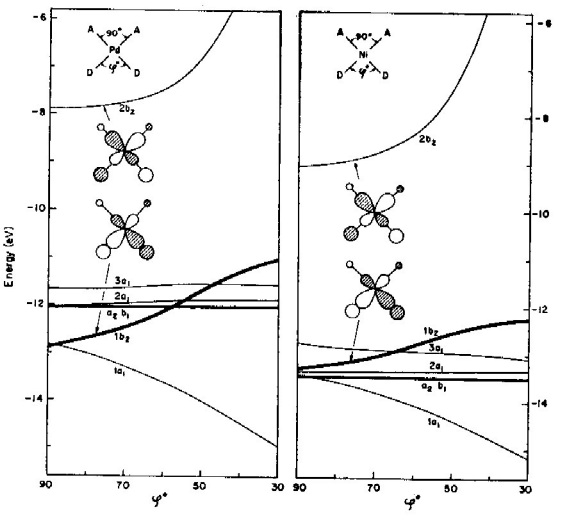

Fig. 4. Computed Walsh diagrams for $PdA_2D_2^{2-}$ (left) and $NiA_2D_2^{2-}$ (right), for decrease of the D-M-D angle φ. The A-M-A angle is kept at 90°. The $2b_2$ orbital is vacant.

The differential $1b_2$ destabilization may arise from two causes - decreasing M-D bonding and increasing D-D antibonding. Either way, it would be anticipated that if the D 1s orbital component in $1b_2$ is large, the destabilization of $1b_2$ will also be large. Indeed the calculated D 1s orbital contribution in $1b_2$ is 54% for Pd and 38% for Ni at $\omega=90°$, which accords with the larger destabilization of the Pd $1b_2$ level.

There is another way of analyzing this effect. The $1b_2$ orbital of MA_2D_2 is constructed in 16 from the antisymmetric D_2 combinations interacting with a bent MA_2 fragment. This interaction carries in it a substantial fraction of the M-D bond energy. Since the resulting $1b_2$ level

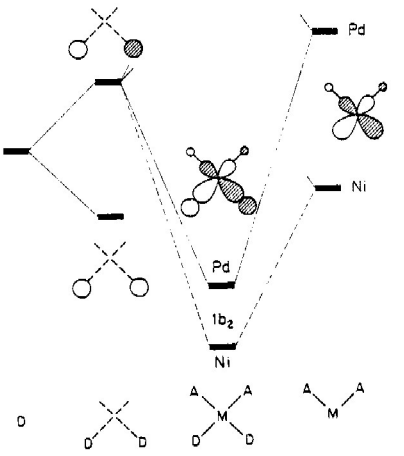

16

of $MA_2D_2^{2-}$ correlates to the b_2 of MA_2 in the D_2 elimination step, a greater energy difference between the $MA_2D_2^{2-}$ b_2 level and the MA_2^{2-} b_2 level would be associated with a greater activation energy for the reaction. The computed energy differences of the b_2 level are 2.1 eV for Pd and 1.3 eV for Ni. This is exactly what would be required to explain the different energy pattern for the Pd and Ni eliminations.

We have assigned the effect to the b_2 levels, but in fact it can be traced deeper. The b_2 level in the MA_2^{2-} fragment left behind is mainly a metal d orbital. It is higher for Pd than for Ni because the Pd and Ni d parameters are in that order. To probe this explanation we performed a numerical experiment in which D_2 was eliminated from a $MA_2D_2^{2-}$, where the M carried the Pd orbitals but with a variable 4d valence state ionization potential. The computed barrier fell monotonically with a decrease in energy of 4d orbitals.

There is a temptation here to correlate the M-D bond strength, formed in part by this b_2 interaction, with increased activation energy to reductive elimination. Some thought about the matter, with the help of diagram 16, shows that the relationship is not so simple. When the A_2M orbital is higher in energy than the antisymmetric combination of D orbitals, a more destabilized MA_2 b_2 would lead to a weaker M-D bond, while at the same time it would give a larger energy gap between b_2 levels of MA_2 and $MA_2D_2^{2-}$. A detailed calculation shows that the overlap population does not increase monotonically with higher Pd 4d energy, but peaks at the position of resonance with the D_2 antisymmetric combination. Thus, the energy gap is not always an index of the thermodynamic stability of an M-D bond, but it can be an index of the "kinetic" stability of $MA_2D_2^{2-}$ to reductive elimination.

Our conclusion: A lower positioning of the ML_2 b_2 orbital in ML_2R_2 facilitates the reductive elimination of R_2. A lower ML_2 b_2 energy will be given by a lower metal d orbital energy.

While our major focus was the difference between Ni and Pd, we have also studied, albeit in abbreviated form, the Pt case. A model $PtA_2D_2^{2-}$ elimination surface gives a barrier slightly higher than in the Pd case. The Pt 5d parameters place it between Ni and Pd, but closer to Pd. The b_2 orbital is 50% on the D_2 ligands at $\theta=90°$, a value again close to that computed for Pd. These theoretical findings are in accord with the experimental observation of difficult reductive elimination from Pt complexes.

The hydride model is extremely useful in unraveling the effect of σ donor or acceptor strength on the ease of the elimination reaction. The detailed analysis, not presented here, leads to two further conclusions: The better the σ-donating capability of the leaving groups, the more readily the elimination reaction proceeds. Also stronger donor ligands which are trans to the leaving groups give a higher barrier for the elimination reaction.

REDUCTIVE ELIMINATION FROM THREE-COORDINATE COMPLEXES

Kinetic studies of cis Pd(II) (2,3) dimethyls and Au(III) trimethyls (4) indicate that elimination is preceded by a dissociative step. The resulting MLR_2 intermediate is a representative of the intriguing d^8 ML_3 class of complexes. The geometrically attractive trigonal planar structure for these molecules turns out to be Jahn-Teller unstable in a low-spin configuration. Distortions to T or Y shaped structures ensue. The structure of the potential energy surface is summarized in 17. Both T and Y shaped structures should be more stable than the trigonal geom-

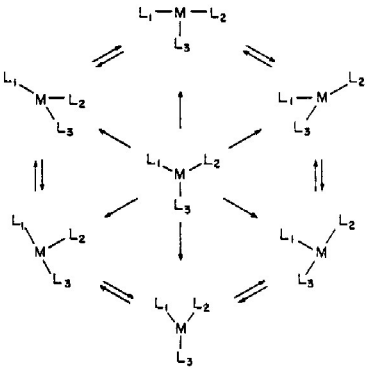

17

etry, but which alternative is the absolute minimum cannot be easily predicted. Whichever conformation is preferred, interconversion of isomeric C_{2v} equilibrium structures (if the ligands differ) is most unlikely to occur through the D_{3h} hill in the middle, but may proceed easily by sweeping through less symmetrical C_s waypoints along the periphery of the Jahn-Teller wheel. Direct structural evidence for deformation of d^8 ML_3 complexes is hard to come by because of the coordinative unsaturation of such 14 electron complexes. If ligand steric bulk is used to stabilize such complexes, one has to worry that the very same ligand property will also perturb the equilibrium geometry from its idealized form. One case where one can see a clear T deformation is for $Rh(PPh_3)_3^+$ (14).

What if the ligand set is substantially asymmetric, as in the $Pd(CH_3)_2(PR_3)_2$ decompositions studied by the Stille and Yamamoto groups? If phosphine dissociation occurs we are led to a three coordinate PdR_2PR_3 complex. The ligand isomerization scheme 17 simplifies to 18. By symmetry the right-hand side of 18 is identical to the left. We will soon present a detailed surface for this polytopal process. For the moment let us assume that the scheme summarizes the experimental possibilities and see how it fits the available experimental data.

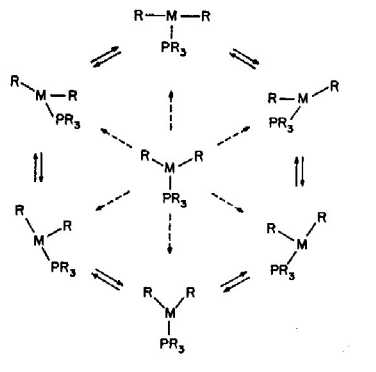

18

Least-motion departure of a phosphine from cis $Pd(CH_3)_2(PR_3)_2$ brings one into a T-shaped entry point in 18, at 4 o'clock. It is easy to imagine a minor rearrangement to the Y-shaped conformer at 6o'clock. This geometry is an obvious exit channel for elimination of R_2. Alternatively elimination could proceed directly from the T-shaped entry point.

Now consider the trans isomer of $Pd(CH_3)_2(PR_3)_2$. Departure of a phosphine leads one into 18 at 12 o'clock. Elimination from there is most unlikely. If the general features of the ML_3 surface were preserved one would nevertheless expect an easy transit around the Jahn-Teller wheel to 6 o'clock, the ethane exit channel. Apparently this does not heppen. Trans dialkyl Pd complexes appear to be quite stable to simple reductive elimination, and instead often undergo β-elimination where that process is possible. Where reductive elimination occurs it is preceded by isomerization to the cis form, assisted either by polar, coordinating solvents (3), or by addition of the cis isomer, in an autocatalytic process (2). Obviously the simple picture of unrestricted motion around the rim of 18 needs modification. Let us investigate the effect of ligand electronic asymmetry on polytopal rearrangements in the three-coordinate manifold.

Again we first employ the hydride model, as we did for the four-coordinate complexes. Thus the d^8 molecules studied were PdD_3^-, $PdDA_2^-$, and $PdAD_2^-$. The characteristic features of the Jahn-Teller surface that we first delineated for $Au(CH_3)_3$ (8a) are preserved in the PdD_3^- surface Fig. 5. A high hill of D_{3h} geometry is in the center surrounded by three descending ridges of Y-shaped geometry. Each of three equivalent T-shaped minima is in a round valley between the two ridges and has two open channels leading to reductive elimination. The activation energy for the elimination is about 0.1eV, while the energy barrier for isomerization from one T-shape to another amounts to 0.4 eV.

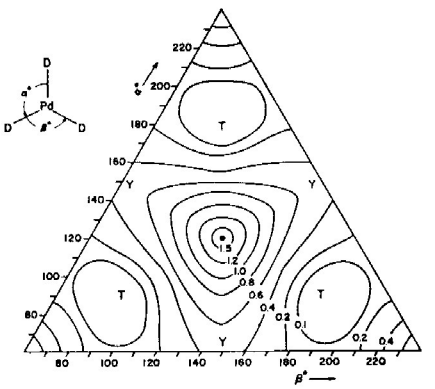

Fig. 5 Potential energy surface calculated for PdD_3^- varying the two D–Pd–D angles α and β. The energies of the contours are in electron volts relative to the T shape.

The topology of the potential surface is explained by orbital diagram 19. The half-filled e' level immediately shows the Jahn-Teller instability of the D_{3h} geometry. When PdD_3^- is dis-

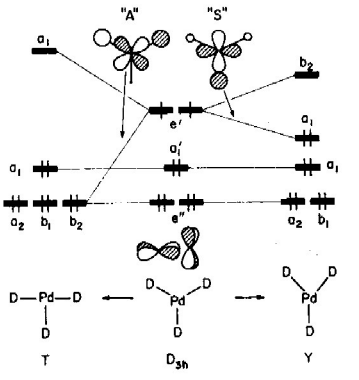

19

torted to a T-shape, one of the e′ components, "A", is stabilized by decreasing Pd-D antibonding interaction and eventually becomes a pure Pd d orbital. On the other hand, the distortion to a Y-shape stabilizes another component, "S" of e′. But it is not by so much, because some Pd-D antibonding character still remains in the "S" component in the Y geometry. This is why the T-shape is more stable than the Y.

Potential surfaces for $PdAD_2^-$ and $PdDA_2^-$ are shown in Fig. 6. $PdAD_2^-$ will be a model for $Pd(PR_3)(CH_3)_2$. In spite of the reduced symmetry, these surfaces maintain the basic electronic properties of the more symmetric PdD_3^-. The trigonal geometry is on a hill, and two kinds of approximate T-shapes are local minima.

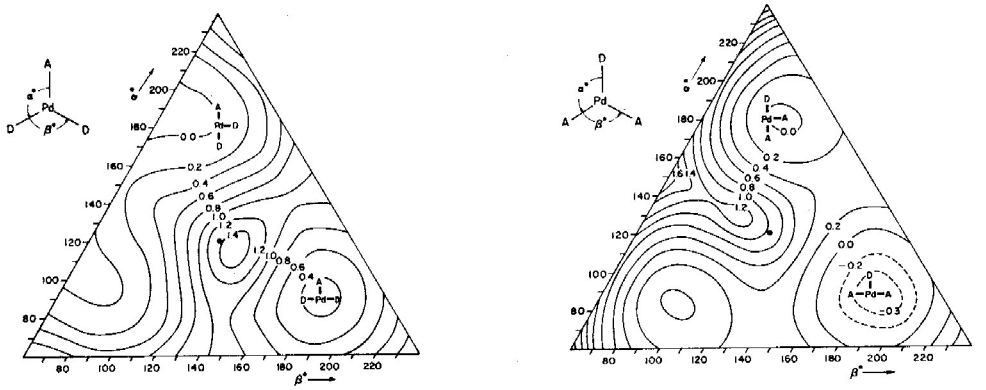

Fig. 6. Potential energy surfaces calculated for $PdAD_2^-$ (left) and $PdDA_2^-$ (right), varying the two angles α(A-Pd-D) and β(D-Pd-D or A-Pd-A). The energies of the contours are in electron volts relative to the T shape in which one wing is occupied by D and another wing by A.

Let us try to understand the relative stability of the T and Y shapes in these less symmetrical systems. We know from 19 that T is basically more stable than Y. What is required is a procedure for evaluating substituent site preferences in T and Y. In the T form the occupied e′ component is "A" (see 19) which has some ligand contribution on the wings of the T and so produces the charge distribution 20. In the Y shape "S" is occupied, and that forces the charge imbalance shown in 21. This is all relative to the trigonal form, where one can think of both orbitals equally occupied, by symmetry the same electron density on all ligands.

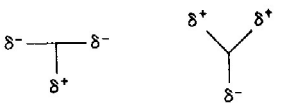

20 21

Now we reason that more electronegative substituents (poorer σ donors, better σ acceptors) will preferentially go where there is an excess of electron density (15). The optimum substitution patterns that follow are presented in 22 and 23. We can now summarize our qualitative expectations for the relative stabilities of the asymmetric T and Y shapes, in Scheme 2. Be-

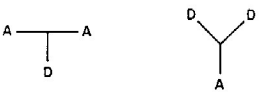

22 23

side some of the structures we place one or more arrows. Each indicates a stabilization, a solid arrow for the inherent greater stability of the T, a dashed arrow for fulfilling to a variable extent, the desired substitution pattern summarized in 22 or 23. There is good qualitative agreement between Scheme 2 and the computed surfaces of Fig. 6.

Scheme 2

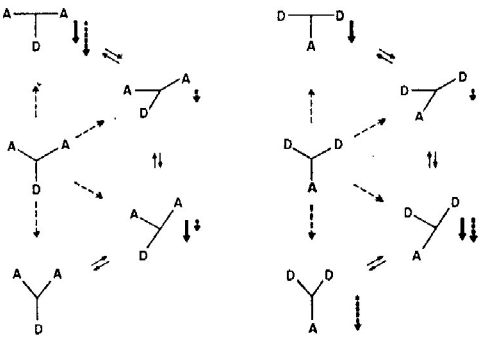

The most interesting consequence of the electronic asymmetry of A and D ligands to be seen from Fig. 6 is the creation of substantial energy barriers to a transit around the Jahn-Teller wheel. The activation energy for going from trans-$PdAD_2^-$ 24 to cis-$PdAD_2^-$, 25, is 0.75 eV, and that for the reverse isomerization is 1.1 eV. Corresponding activation energies for $PdDA_2^-$

24 **25**

are 0.6 eV and 0.3 eV. Thus we conclude: T-shaped trans-$PdLR_2$, which might be produced by liberating L from trans-PdL_2R_2, will encounter a substantial energy barrier to rearrangement to cis-$PdLR_2$, which has an open channel for reductive elimination of R_2; and: When the leaving groups are poor donors, cis-trans isomerization between two T-shaped geometries should be much easier than elimination of A_2. If R is a strong σ donor and L is a poor donor or an acceptor then the rearrangement from the trans-derived three-coordinate structure to the cis-derived one (motion from 12 o'clock to 4 in 18) will not be facile.

These are model calculations. They were supported by detailed examination of a surface for valence tautomerism in $Pd(PH_3)(CH_3)_2$, Fig. 7. P-Pd-C angles α and C-Pd-C angle β are var-

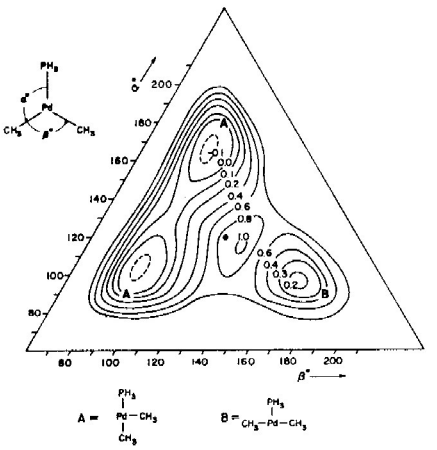

Fig. 7. Potential energy surface calculated for Pd-$(PH_3)(CH_3)_2$ varying the two angles α(P-Pd-C) and β(C-Pd-C). The energies of the contours are in electron volts relative to the T shape defined by A below the triangle.

ied. Note the presence of three T-shaped minima, and an activation energy of 0.5 eV for the trans→cis $Pd(PH_3)(CH_3)_2$ isomerization and 0.8 eV for the reverse reaction. Further calculations indicate that elimination can occur directly from a T-geometry and need not ascend to a Y-shaped locus.

We have not yet mentioned the most interesting feature of Fig. 7. It is the prediction of a most easy motion between the two A type minima, 26a and b. To put it into other words the

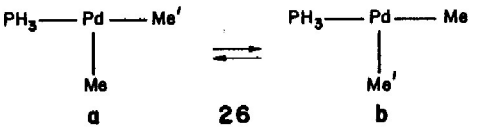

cis methyl groups in this complex can interchange their positions, without passing through either a trigonal geometry or a trans isomer. This is precisely what has been observed in labelling experiments in the thermal decomposition of $(PEt_3)_2Pt(C_2H_5)_2$ by McCarthy, Nuzzo and Whitesides (16).

THE NICKELACYCLOPENTANE SYSTEM

Reductive elimination is often only one of several reaction channels open to an organometallic complex. A beautiful example of the richness of one such system is to be found in the chemistry of nickelacyclopentanes, which R. J. McKinney, D. L. Thorn, A. Stockis and I have studied theoretically (10b).

Following pioneering studies from the Whitesides group (5a), a substantive contribution to our mechanistic understanding of nickelacyclopentane reactions was made by Grubbs and co-workers on the nickelacyclopentane system with tert-phosphine ligands (1). A summary of their studies is shown in Scheme 3. Nickelacyclopentanes of coordination number three, four, and five are in equilibrium with each other. For each complex there is a dominant reaction channel: the three-coordinate complex 27 yields butene, the four-coordinate complex 28 reductively eliminates cyclobutane, and the five-coordinate metallacycle 29 reductively fragments to give ethylene. Furthermore, kinetic evidence points to an equilibrium between 29 and $L_2Ni(CH_2)_4$, complex 30, different from 28, preceding the ethylene forming step.

Scheme 3

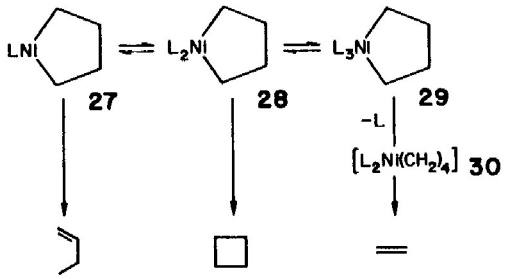

The reaction scheme is significantly simplified by these findings. Nevertheless numerous mysteries remain. A partial list of these includes the detailed mechanism of butene formation, the degree of concert in the cyclobutane- and ethylene-forming steps, the nature of the bisphosphine complex 30, and the fate of the metal fragments in the reactions. More generally one would like to understand the way in which ligand number and geometrical disposition influence the mode of degradation of these d^8 complexes. The complexity of several possible multistep pathways for butene formation led us to exclude it from our theoretical study. However we will attempt to shed some light on the other questions. A previous study had already explored the relationship of some d^8 iron metallacyclopentane derivatives with bis-olefin complexes (17).

The central importance of the four-coordinate metallacycles, both from the synthetic viewpoint, as well as the undefined nature of 30, led us to begin by exploring the potential energy surface

of bis-phosphine metallacycle complexes. Characteristic of four-coordinate Ni(II) complexes is a facile equilibrium between low-spin square planar and high-spin tetrahedral structures. This suggests immediately the geometrical alternatives 31 and 32. Indeed these are important structures, but an unexpected contender, possessing a "trans" geometry, 33, turned up when we examined some modifications of the "tetrahedral" structure 32.

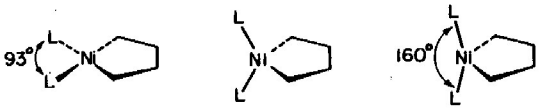

Our search for stable points on the four-coordinate metallacycle surface utilized two degrees of freedom. As defined in 34, these are the L-Ni-L (L=PH_3) angle θ and the torsion angle between P-Ni-P and C-Ni-C planes α. At α=90°, we calculated a Walsh diagram for varying the

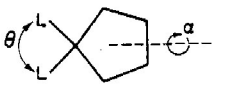

P-Ni-P angle θ. Fig. 8 shows the d block as θ is varied. Indeed there is a typical tetrahed-

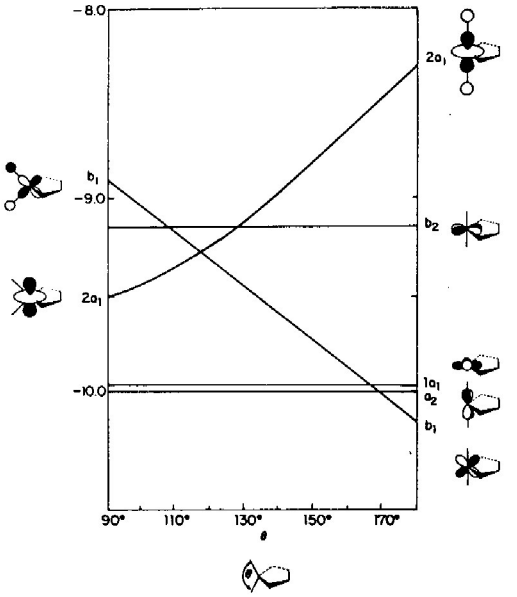

Fig. 8. A Walsh diagram for varying the interligand angle θ in $Ni(PH_3)_2(CH_2)_4$, for α=90° (see 34). Only d-block orbitals are included.

al ligand field splitting, two levels below three near the geometry that best approximates the tetrahedron $\theta \sim 110°$. There will be three configurations, I-III, competing to be the lowest

$$\text{I} \quad (a_2)^2(1a_1)^2(2a_1)^2(b_2)^1(b_1)^1 \qquad 1,^3A_2$$

$$\text{II} \quad (a_2)^2(1a_1)^2(b_1)^2(2a_1)^1(b_2)^1 \qquad 1,^3B_2$$

$$\text{III} \quad (a_2)^2(1a_1)^2(b_2)^2(2a_1)^1(b_1)^1 \qquad 1,^3B_1$$

triplet, and presumably the ground state of the "tetrahedral" geometry.

The three competing low spin configurations, IV-VI, all have $^1A_1$ state symmetry, and no doubt will mix substantially, especially at intermediate θ. But each configuration will have its own geometrical preferences, with IV favoring low θ, V intermediate θ, and VI high θ.

IV $(a_2)^2(1a_1)^2(2a_1)^2(b_2)^2$ $^1A_1$

V $(a_2)^2(1a_1)^2(2a_1)^2(b_1)^2$ $^1A_1$

VI $(a_2)^2(1a)^2(b_1)^2(b_2)^2$ $^1A_1$

These geometrical preferences arise from the marked change of two of the energy levels with θ. A substantial energy gap at high θ results from the falling slope of the b_1 level, 35, which is stabilized with increasing θ.

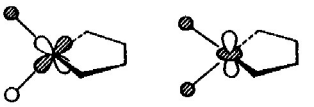

35 **36**

A deficiency of the extended Hückel method, which carries over to the method used here, is that only configuration energies, not state energies, can be calculated. Electron interaction is not explicitly included in our calculations. Configurations I-III will separate into higher-lying singlets and lower-lying triplets. Fig. 9 summarizes the dependence of the configura-

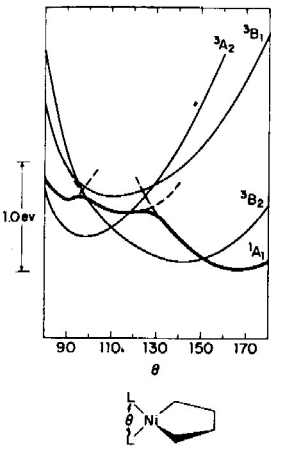

Fig. 9. Approximate changes in state energies of $Ni(PH_3)_2(CH_2)_4$ with the interligand angle θ. The energy of the $^1A_1$ state, relative to the triplet states, is assumed. Energies of the triplet states are taken directly from calculations performed with the appropriate configurations.

ation energies of the triplets upon θ. Also shown are the energies for configurations IV-VI, all of the same symmetry, which will mix to give a single low-lying surface favoring high θ, as indicated by the bold-faced line in Fig. 9. Of the states arising from configurations I-VI, it is likely that four will be at low energy, with preferred values of θ=100° ($^3A_2$), 115° ($^3B_1$)135° ($^3B_2$), and 160° ($^1A_1$). This spin-paired $^1A_1$ species with essentially trans phosphines is the unexpected contender 33.

All that is for the "tetrahedral" isomers. How do these curves connect up to the square planar singlet? A correlation diagram for twisting, i. e. changing α in 34 for any θ may be constructed from symmetry arguments. It is shown for $\theta \sim 90°$, in Figure 10.

The ground state of the square planar form, $^1A_1$, correlates to configuration IV or V of the "tet-

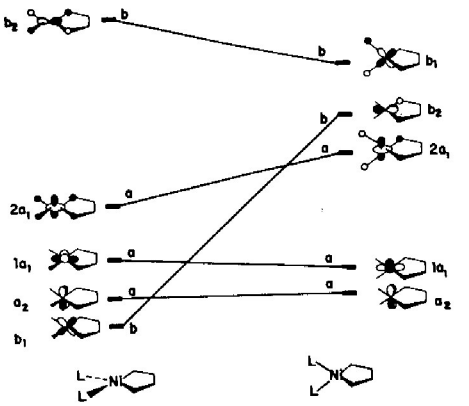

Fig. 10. A correlation diagram for the interconversion of the square-planar form (left) of $Ni(PH_3)_2(CH_2)_4$ with a "tetrahedral" form (right) with $\theta = 90°$. C_2 symmetry is imposed throughout.

rahedral" geometry, depending on θ, but it cannot correlate to configuration VI. While configurations IV, V, and VI will all mix, configuration VI will dominate the $1A_1$ wave function, and it can be said that the direct interconversion of the trans structure 33 and the square planar structure 31 is a forbidden reaction.

A complete elucidation of the intricacies of this potential energy surface will have to await more sophisticated calculations. For the present we propose that five states merit consideration: a ground state square planar singlet, 31 ($1A_1$), three tetrahedral triplets, 32 ($3A_2$, $3B_1$, $3B_2$), and a novel singlet, 33 ($1A_1$), a "trans" isomer which is neither square planar nor tetrahedral.

In the next stage of our study (see Ref. 8b for details) we considered several degradation modes of the metallacycle. It was found (Scheme 4) that allowed reactions lead from 31 to cyclobutane, and from 33 to two olefins, with or without passing through a tetrahedral intermediate

Scheme 4

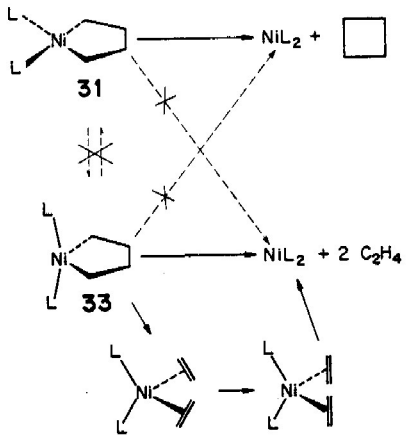

in which the olefins are bound, whereas it is forbidden for 31 to fragment to ethylene and 33 to eliminate cyclobutane. In fact this is a general trend throughout our study: If metallacycle degradation to form cyclobutane is symmetry-allowed, then the formation of ethylene will usually be symmetry-forbidden, and vice versa.

The metallacycle reactions, cyclobutane or ethylene formation, are formally "reductive elimination" processes. However, the formation of cyclobutane requires that the electron pair be transferred to the metal center via an orbital of b_2 symmetry, whereas the formation of two ethylene molecules takes place with electrons being transferred to the metal center via an a_1 orbital. That this should be so is graphically illustrated in Fig. 11. In these d^8 complexes there is only one empty d orbital which, depending upon the geometry and coordination number, may be of a_1 or b_2 symmetry. Consequently, either cyclobutane or ethylene formation, but never both, will be an allowed reaction from any specified symmetrical geometry of the metallacycle complex.

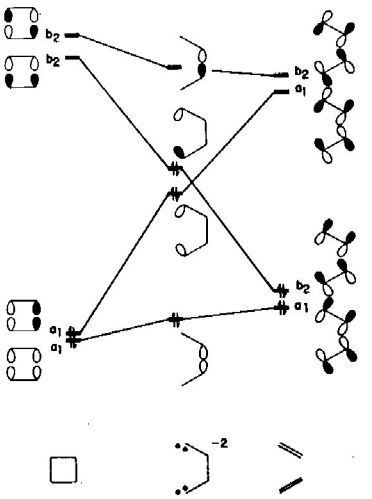

Fig. 11. A schematic diagram illustrating the evolution of the orbitals of a $(CH_2)_4$ fragment. In the center is a tetramethylene dianion which is transformed into cyclobutane (left) or two ethylenes (right) with loss of two electrons.

The preceding discussion has focused on but a small part of the nickelacyclopentane surface. Fragmentations of the three- and five-coordinate metallacycle are particularly intricate and receive the attention they deserve in our full paper on the subject (10b).

Acknowledgement - The research described in this contribution was the product of a fruitful collaboration with Tom Albright, Kazuyuki Tatsumi and Armel Stockis at Cornell, Jay Kochi and Sanshiro Komiya at Indiana, Akio Yamamoto at the Tokyo Institute of Technology, John Stille at Colorado State, Ron McKinney and Dave Thorn at duPont. Their inspiration and help is most gratefully acknowledged. The work at Cornell was generously supported by the National Science Foundation through Research Grant CHE 7828048.

REFERENCES

1. R. H. Grubbs and A. Miyashita, J. Am. Chem. Soc. 100, 7416-7418 (1978), and references therein.
2. F. Ozawa, T. Ito, and A. Yamamoto, Ibid., 102, 6457-6463 (1980), and references therein.
3. A. Gillie and J. K. Stille, Ibid., 102, 4933-4941 (1980), and references therein.
4. S. Komiya, T. A. Albright, R. Hoffmann, and J. K. Kochi, Ibid., 98, 7255-7265 (1980), and references therein.
5. (a) G. M. Whitesides, Pure Appl. Chem. 53, 287-292 (1981) and references therein.
   (b) S. Komiya, A. Yamamoto, and T. Yamamoto, Chem. Lett. 1273-1276 (1978).
6. M. P. Brown, R. J. Puddephatt, and C. E. Upton, J. Chem. Soc. Dalton Trans. 2457-2465 (1974).
7. R. Romeo, D. Minniti and S. Lanza, Inorg. Chem. 18, 2362-2368 (1979) and references therein.
8. See G. K. Anderson and R. J. Cross, Chem. Soc. Revs. 185-215 (1980) and references therein.
9. T. Yamamoto, A. Yamamoto, and S. Ikeda, J. Am. Chem. Soc. 93, 3360-3364 (1971), and references therein.
10.(a) Ref. 4 and S. Komiya, T. A. Albright, R. Hoffmann and J. K. Kochi, Ibid., 99, 8440-

8447 (1977).
(b) R. J. McKinney, D. L. Thorn, R. Hoffmann, A. Stockis, Ibid., 103, 2595-2603(1981)
(c) K. Tatsumi, R. Hoffmann, A. Yamamoto and J. K. Stille, Bull. Chem. Soc. Jpn., in press.
11. For other theoretical work on reductive elimination see:
(a) R. G. Pearson, Symmetry Rules for Chemical Reactions, p. 286, 405, Wiley-Interscience, New York (1976).
(b) P. S. Braterman and R. J. Cross, Chem. Soc. Rev. 2, 271-294 (1973).
(c) B. Åkermark and A. Ljungqvist, J. Organomet. Chem. 182, 59-75 (1979); B. Åkermark, H. Johansen, B. Roos and U. Wahlgren, J. Am. Chem. Soc. 101, 5876-5883 (1979).
12. For some leading references on the theory of the reverse reaction, oxidative addition, see A. Dedieu and A. Strich, Inorg. Chem. 18, 2940-2943 (1979); A. Sevin, Nouv. J. Chim. 5, 233-241 (1981).
13. See also R. Hoffmann, B. F. Beier, E. L. Muetterties, and A. R. Rossi, Inorg. Chem. 16, 511-522 (1977).
14. Y. W. Yared, S. L. Miles, R. Bau, and C. A. Reed, J. Am. Chem. Soc. 99, 7076-7078 (1977).
15. This type of argument has been successfully used by us before: R. Hoffmann, J. M. Howell, and E. L. Muetterties, Ibid., 94, 3047-3058 (1972).
16. T. J. McCarthy, R. G. Nuzzo, and G. M. Whitesides, Ibid., 103, 1676-1678 (1981).
17. A. Stockis and R. Hoffmann, Ibid., 102, 2952-2962 (1980).